Advances in Applied Mathematics and Mechanics
Adv. Appl. Math. Mech., Vol. **5**, No. 4, pp. 461-476

DOI: 10.4208/aamm.13-13S05
August 2013

Alternating Direction Implicit Orthogonal Spline Collocation on Non-Rectangular Regions

Bernard Bialecki[1,*] and Ryan I. Fernandes[2]

[1] *Department of Applied Mathematics and Statistics, Colorado School of Mines, Golden, CO 80401, USA*
[2] *Department of Mathematics, The Petroleum Institute, Abu Dhabi, United Arab Emirates*

Received 25 June 2012; Accepted (in revised version) 8 September 2012

Available online 7 June 2013

Dedicated to Professor Graeme Fairweather in honor of his 70^{th} birthday.

Abstract. The alternating direction implicit (ADI) method is a highly efficient technique for solving multi-dimensional time dependent initial-boundary value problems on rectangles. When the ADI technique is coupled with orthogonal spline collocation (OSC) for discretization in space we not only obtain the global solution efficiently but the discretization error with respect to space variables can be of an arbitrarily high order. In [2], we used a Crank Nicolson ADI OSC method for solving general nonlinear parabolic problems with Robin's boundary conditions on rectangular polygons and demonstrated numerically the accuracy in various norms. A natural question that arises is: Does this method have an extension to non-rectangular regions? In this paper, we present a simple idea of how the ADI OSC technique can be extended to some such regions. Our approach depends on the transfer of Dirichlet boundary conditions in the solution of a two-point boundary value problem (TPBVP). We illustrate our idea for the solution of the heat equation on the unit disc using piecewise Hermite cubics.

AMS subject classifications: 65M70

Key words: Alternating direction implicit method, orthogonal spline collocation, two point boundary value problem, Crank Nicolson, parabolic equation, non-rectangular region.

1 Introduction

ADI methods were first introduced in the context of finite differences (FD) by Peaceman and Rachford [9] for solving elliptic and parabolic differential equations. Over the past

*Corresponding author.
Email: bbialeck@mines.edu (B. Bialecki), rfernandes@pi.ac.ae (R. I. Fernandes)

70 years the ADI technique has been coupled with finite element Galerkin (FEG) and OSC discretizations in space for solving efficiently a variety of multi-dimensional time dependent initial-boundary value problems on rectangles, see [7] and references therein for a brief overview of ADI FEG and ADI OSC methods.

For over 20 years, we have been developing and analysing new ADI OSC methods for solving linear and nonlinear time dependent problems on rectangles and rectangular polygons. In [1], we formulated and analyzed a Crank Nicolson ADI OSC method for the solution of general linear parabolic problems with Dirichlet boundary conditions on rectangles. In [2], we formulated a Crank Nicolson ADI OSC method to solve general nonlinear parabolic problems with Robin's boundary conditions on rectangular polygons. The merits of these schemes and comparisons with ADI FD and ADI FEG methods have been discussed in [7]. A natural question that arises is: Does the ADI OSC technique have an extension to non-rectangular regions such as a triangle, a disc, a quadrilateral, etc? The purpose of this paper is to present a simple idea of how the ADI OSC technique can be extended to some such regions. Our approach depends on the transfer of Dirichlet boundary conditions in the solution of TPBVP on the original interval without the end subintervals of a non-uniform partition. We present our idea for the solution of the heat equation on the unit disc in space using piecewise Hermite cubics in the space coordinate directions.

A brief outline of the paper is as follows. In Section 2 we consider solution of TPBVP on the original interval without the end subintervals. In Section 3 the ADI OSC method for a unit disc is explained and numerical results, demonstrating the optimal rate of convergence in the maximum norm, are presented. Concluding remarks are given in Section 4.

2 OSC for TPBVP without end subintervals

Consider the TPBVP on $[a,b]$ with Dirichlet boundary conditions

$$Lu=f(x), \quad x\in(a,b), \quad u(a)=u_a, \quad u(b)=u_b, \tag{2.1}$$

where a, b, u_a, u_b are given numbers, $a<b$, f is a given function on (a,b), and, with r a given nonnegative function on (a,b),

$$Lu=-u''+r(x)u. \tag{2.2}$$

Assume that N is a natural number, $\{x_i\}_{i=0}^N$ is, in general, a nonuniform partition of $[a,b]$, that is,

$$a=x_0<x_1<\cdots<x_{N-1}<x_N=b.$$

Observe that there are N subintervals corresponding to the partition $\{x_i\}_{i=0}^N$. We want to approximate u of (2.1)-(2.2) on $[x_1,x_{N-1}]$ rather than $[x_0,x_N]$; see Fig. 1.

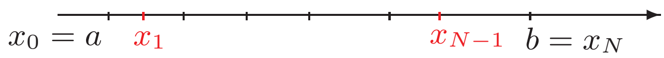

Figure 1: Partition.

Let V be the space of piecewise Hermite cubics on $[x_1,x_{N-1}]$ defined by

$$V=\{v\in C^1[x_1,x_{N-1}]:\ v|_{[x_i,x_{i+1}]}\in P_3,\ i=1,\cdots,N-2\},$$

where P_3 is the set of polynomials of degree ≤ 3.

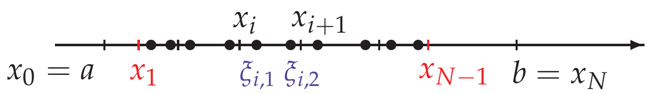

Figure 2: Collocation points.

In each $[x_i,x_{i+1}]$, $i=1,\cdots,N-2$, let $\xi_{i,1}$, $\xi_{i,2}$ (see black dots in Fig. 2) be two collocation (Gauss) points given by

$$\xi_{i,1}=x_i+\frac{3-\sqrt{3}}{6}(x_{i+1}-x_i),\quad \xi_{i,2}=x_i+\frac{3+\sqrt{3}}{6}(x_{i+1}-x_i). \tag{2.3}$$

We look for the approximate solution $U\in V$ such that

$$LU(\xi_{i,k})=f(\xi_{i,k}),\quad i=1,\cdots,N-2,\quad k=1,2. \tag{2.4}$$

Since dim $V=2N-2$ and the number of equations in (2.4) is $2N-4$, we require two additional equations. In order to define these equations, assume that p and q in P_3 satisfy respectively the following interpolation conditions

$$p(a)=u_a,\qquad p(\xi_{1,1})=U(\xi_{1,1}),\qquad p(\xi_{1,2})=U(\xi_{1,2}),\qquad p(x_2)=U(x_2), \tag{2.5a}$$
$$q(x_{N-2})=U(x_{N-2}),\quad q(\xi_{N-2,1})=U(\xi_{N-2,1}),\quad q(\xi_{N-2,2})=U(\xi_{N-2,2}),\quad q(b)=u_b. \tag{2.5b}$$

Fig. 3 shows that p of (2.5a) interpolates at four points around x_1 and q of (2.5b) interpolates at four points around x_{N-1}.

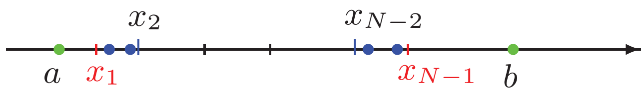

Figure 3: Interpolating points.

It is easy to see that

$$p(x)=u_ap_1(x)+U(\xi_{1,1})p_2(x)+U(\xi_{1,2})p_3(x)+U(x_2)p_4(x), \tag{2.6}$$

and

$$q(x)=U(x_{N-2})q_1(x)+U(\xi_{N-2,1})q_2(x)+U(\xi_{N-2,2})q_3(x)+u_bq_4(x), \tag{2.7}$$

where the p_i and q_i are cardinal functions, each of which in P_3 is associated with one particular interpolation point used in the definitions (2.5a) and (2.5b) of p and q, respectively. For example, p_1 is associated with the interpolation point a and

$$p_1(a)=1, \quad p_1(\xi_{1,1})=0, \quad p_1(\xi_{1,2})=0, \quad p_1(x_2)=0.$$

The remaining p_i and the q_i are defined similarly. Each p_i and q_i is easily obtained using Newton's divided difference formula for the Lagrange interpolating polynomial. Our two additional equations, complementing (2.4), are

$$U(x_1)=p(x_1), \quad U(x_{N-1})=q(x_{N-1}), \tag{2.8}$$

which, on using (2.6) and (2.7), yield respectively

$$U(x_1)-p_2(x_1)U(\xi_{1,1})-p_3(x_1)U(\xi_{1,2})-p_4(x_1)U(x_2)=u_ap_1(x_1) \tag{2.9}$$

and

$$\begin{aligned}&-q_1(x_{N-1})U(x_{N-2})-q_2(x_{N-1})U(\xi_{N-2,1})-q_3(x_{N-1})U(\xi_{N-2,2})\\&+U(x_{N-1})=u_bq_4(x_{N-1}).\end{aligned} \tag{2.10}$$

To describe the algebraic problem corresponding to (2.4), (2.9) and (2.10), we write the approximate solution

$$U(x)=\sum_{i=1}^{N-1}[c_{2i-1}v_i(x)+c_{2i}s_i(x)], \quad x\in[x_1,x_{N-1}], \tag{2.11}$$

where the v_i and s_i in V_h are respectively the value and scaled slope basis functions associated with the partition point x_i. Substitution of (2.11) into (2.9), (2.4), and (2.10) gives rise to the $(2N-2)\times(2N-2)$ linear system

$$A\mathbf{c}=\mathbf{f}, \tag{2.12}$$

where

$$\mathbf{c}=[c_1,c_2,\cdots,c_{2N-3},c_{2N-2}]^T, \quad \mathbf{f}=[f_1,f_2,\cdots,f_{2N-3},f_{2N-2}]^T,$$

and the entries of **f** are given in terms of u_a, $f(\xi_{i,k})$, $i=1,\cdots,N-2$, $k=1,2$, and u_b. It follows from formulas (5.1)-(5.3) in [1] defining the v_i and s_i that v_1 and s_1 are zero outside the interval $[x_1,x_2]$, for $i=2,\cdots,N-2$, v_i and s_i are zero outside the interval $[x_{i-1},x_{i+1}]$, and v_{N-1} and s_{N-1} are zero outside the interval $[x_{N-2},x_{N-1}]$. Therefore, the matrix A has the following structure, displayed here for $N=6$,

$$A=\begin{bmatrix} \times & \times & \times & \times & & & & & & \\ \times & \times & \times & \times & & & & & & \\ \times & \times & \times & \times & & & & & & \\ & & \times & \times & \times & \times & & & & \\ & & \times & \times & \times & \times & & & & \\ & & & & \times & \times & \times & \times & & \\ & & & & \times & \times & \times & \times & & \\ & & & & & & \times & \times & \times & \times \\ & & & & & & \times & \times & \times & \times \\ & & & & & & \times & \times & \times & \times \end{bmatrix}.$$

The system (2.12) can be solved at a cost $\mathcal{O}(N-2)$ using the capacitance matrix method [3] and the package COLROW [4, 5]. To describe this computation, we consider the matrix B whose rows are the same as the corresponding rows in A, except that the first and last rows of B are

$$[1,0,\cdots,0,0,0,0], \quad [0,0,\cdots,0,0,1,0],$$

respectively. These two rows correspond to specifying U of (2.11) at x_1 and x_{N-1}, respectively. The matrix B is almost block diagonal (ABD) [4] and nonsingular [6] since the function r in (2.2) is nonnegative. A linear system with B can be solved at a cost $\mathcal{O}(N-2)$ using the package COLROW of [4, 5] for solving ABD linear systems. We look for the solution $\mathbf{c}$ of (2.12) in the form

$$\mathbf{c}=\mathbf{d}+\gamma_1\mathbf{d}_1+\gamma_2\mathbf{d}_2, \tag{2.13}$$

where the numbers γ_1 and γ_2 are to be determined and the vectors $\mathbf{d}$, $\mathbf{d}_1$, $\mathbf{d}_2$ are solutions of the linear systems

$$B\mathbf{d}=[0,f_2,\cdots,f_{2N-3},0]^T, \quad B\mathbf{d}_1=[1,0,\cdots,0,0]^T, \quad B\mathbf{d}_2=[0,0,\cdots,0,1]^T. \tag{2.14}$$

Using

$$A(i,:)=B(i,:), \quad i=2,\cdots,2N-3,$$

and (2.14) it is easy to verify that, for arbitrary γ_1 and γ_2,

$$A(i,:)(\mathbf{d}+\gamma_1\mathbf{d}_1+\gamma_2\mathbf{d}_2)=f_i, \quad i=2,\cdots,2N-3.$$

Moreover,

$$A(i,:)(\mathbf{d}+\gamma_1\mathbf{d}_1+\gamma_2\mathbf{d}_2)=A(i,:)\mathbf{d}+\gamma_1 A(i,:)\mathbf{d}_1+\gamma_2 A(i,:)\mathbf{d}_2, \quad i=1,2N-2.$$

Hence $\mathbf{c}$ given by the right-hand side of (2.13) solves (2.12) if and only if γ_1 and γ_2 solve the 2×2 linear system

$$\begin{bmatrix} A(1,:)\mathbf{d}_1 & A(1,:)\mathbf{d}_2 \\ A(2N-2,:)\mathbf{d}_1 & A(2N-2,:)\mathbf{d}_2 \end{bmatrix}\begin{bmatrix}\gamma_1\\ \gamma_2\end{bmatrix}=\begin{bmatrix} f_1 \\ f_{2N-2}\end{bmatrix}-\begin{bmatrix} A(1,:)\mathbf{d} \\ A(2N-2,:)\mathbf{d}\end{bmatrix}. \tag{2.15}$$

Since A and B are nonsingular, it follows from Theorem 1 in [3] that the 2×2 matrix in (2.15) is also nonsingular. Thus we obtain solution $\mathbf{c}$ of the system (2.12) by first computing, with the use of COLROW, the vectors $\mathbf{d}$, $\mathbf{d}_1$, and $\mathbf{d}_2$ of (2.14). Then we set up and solve the system (2.15) and finally we form $\mathbf{c}$ using (2.13). The cost of this computation is $\mathcal{O}(N-2)$.

Numerical tests indicate that the proposed OSC scheme, comprising (2.4) and (2.8), for approximating u of (2.1)-(2.2) is fourth order accurate in the maximum norm over $[x_1,x_{N-1}]$. As a test example, we take $[a,b]=[-1,1]$, $u(x)=e^x$, and $r(x)=1$. For an even natural number N, we use the nonuniform partition $\{x_i\}_{i=0}^N$ of $[-1,1]$ defined by

$$-x_i=x_{N-i}=\cos(i\pi/N), \quad i=0,\cdots,N/2. \tag{2.16}$$

We compute the maximum norm error in U on $[x_1,x_{N-1}]$ using 10 points in each subinterval $[x_i,x_{i+1}]$. We expect $\mathcal{O}(h^4)$ accuracy, where

$$h=\max_{i=1,\cdots,N-2}(x_{i+1}-x_i).$$

Drawing, in the xy plane, half of the unit circle with the endpoints $(-1,0)$ and $(1,0)$, dividing it into N equal subarcs, and using $x_{N/2}=0$, we see that

$$h=x_{N/2+1}-x_{N/2}=\sin(\pi/N)\approx\pi/N \text{ for large } N. \tag{2.17}$$

For several values of N, denoted by N_i, and the corresponding values of h, denoted by h_i, we compute the convergence rate using the formula

$$\text{Rate}=\log(\epsilon_i/\epsilon_{i+1})/\log(h_i/h_{i+1}), \tag{2.18}$$

where ϵ_i is the error corresponding to N_i. The obtained results, presented in Table 1, indicate the expected convergence rate of 4.

Table 1: Errors and rates.

	$\vert u-U\vert$	
N_i	Error	Rate
10	2.07–05	
20	1.55–06	3.806
30	3.08–07	4.004
40	9.82–08	3.985
50	4.03–08	4.001

In what follows, we refer to the two additional equations in (2.8) as transferring of the Dirichlet boundary conditions at a and b (see green dots in Fig. 4) to x_1 and x_{N-1} (see red dots in Fig. 4).

The equations in (2.8) are not the only choice of two additional equations complementing (2.4). It is possible, for example, to use the following two equations

$$U'(x_1)=p'(x_1), \quad U'(x_{N-1})=q'(x_{N-1}), \tag{2.19}$$

Figure 4: Transfer.

where p and q in P_3 satisfy the following interpolation conditions

$$\begin{array}{llll} p(a)=u_a, & p(x_1)=U(x_1), & p(x_2)=U(x_2), & p'(x_2)=U'(x_2), \\ q(x_{N-2})=U(x_{N-2}), & q'(x_{N-2})=U'(x_{N-2}), & q(x_{N-1})=U(x_{N-1}), & q(b)=u_b. \end{array}$$

Again numerical tests (not shown here) indicate that the OSC scheme consisting of (2.4) and (2.19) is fourth order accurate in the maximum norm over $[x_1,x_{N-1}]$.

3 ADI OSC for parabolic problems on the unit disc

Assume that Ω is the open unit disc, that is,

$$\Omega=\{(x,y):x^2+y^2<1\},$$

and $\partial\Omega$ is the boundary of Ω, that is,

$$\partial\Omega=\{(x,y):x^2+y^2=1\}.$$

Let Δ be the Laplace operator. Consider the parabolic problem consisting of the heat equation

$$u_t-\Delta u=f(x,y,t), \quad (x,y,t)\in\Omega\times(0,T], \tag{3.1}$$

the initial condition

$$u(x,y,0)=g_1(x,y), \quad (x,y)\in\overline{\Omega}, \tag{3.2}$$

and the Dirichlet boundary condition

$$u(x,y,t)=g_2(x,y,t), \quad (x,y,t)\in\partial\Omega\times(0,T], \tag{3.3}$$

where f,g_1 and g_2 are given functions.

3.1 Partitions; collocation points

For an even natural number N, we construct a partition of Ω as follows. We divide the unit circle into $2N$ equal subarcs using points $\{P_i\}_{i=0}^{2N}$ with $P_0=P_{2N}=(0,1)$ (see Fig. 5(a)). Vertical and horizontal lines passing through the points P_i (see Fig. 5(a)) give nonuniform partitions $\{x_i\}_{i=0}^{N}$ and $\{y_j\}_{j=0}^{N}$ of $[-1,1]$ along the x and y axes, respectively (see Fig. 5(b)). Note that the x_i are given by (2.16) and that $y_j=x_j$, $j=0,\cdots,N$.

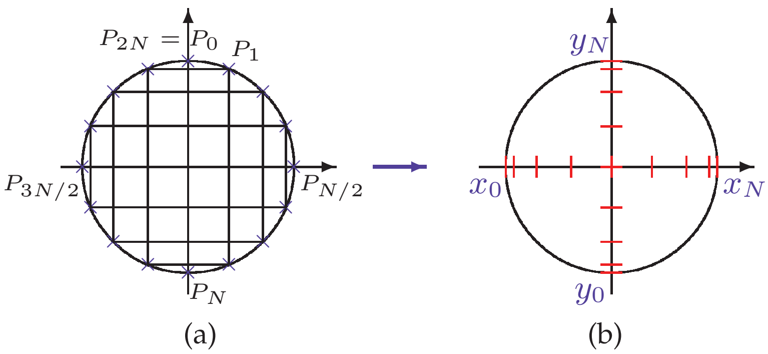

Figure 5: Consistent partition.

The obtained partition of Ω is consistent in the following sense. Let R_x be the union of all vertical lines passing through the points $(x_i,0)$, $i=0,\cdots,N$, and let R_y be the union of all horizontal lines passing through the points $(0,y_j)$, $j=0,\cdots,N$. Then (see Fig. 5(a))

$$R_x\cap\partial\Omega=R_y\cap\partial\Omega.$$

It is possible to obtain other consistent partitions of Ω. For example, with an even natural number N, another consistent partition of Ω is obtained using the uniform partition $\{x_i\}_{i=0}^N$ of $[-1,1]$ given by

$$x_i=-1+2i/N, \quad i=0,\cdots,N,$$

and the corresponding nonuniform partition $\{y_j\}_{j=0}^N$ of $[-1,1]$ given by

$$y_j=-y_{N-j}, \quad y_{N-j}=\sqrt{1-(2j/N)^2}, \quad j=0,\cdots,N/2; \tag{3.4}$$

see Fig. 6.

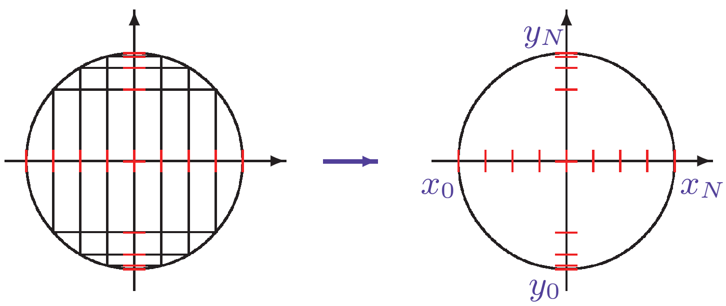

Figure 6: Consistent partition.

In the rest of this Section we use only the consistent partition shown in Figs. 5(a), (b) to describe the ADI OSC method. In each subinterval $[x_i,x_{i+1}]$, $i=1,\cdots,N-2$, there are two collocation points $\xi_{i,1}$ $\xi_{i,2}$ (cf. (2.3)) and similarly, in each subinterval $[y_j,y_{j+1}]$,

$j=1,\cdots,N-2$, there are two collocation points $\eta_{j,1}$ $\eta_{j,2}$ (see black dots in Fig. 7(a)). We have the closed rectangular polygon P_Ω inside $\overline{\Omega}$ given by

$$P_\Omega=\Big\{\bigcup_{i,j=1,\cdots,N-2}[x_i,x_{i+1}]\times[y_j,y_{j+1}]:[x_i,x_{i+1}]\times[y_j,y_{j+1}]\subset\overline{\Omega}\Big\}, \tag{3.5}$$

and four collocation (Gauss) points of the form $(\xi_{i,k},\eta_{j,l})$ in each cell of P_Ω (see black dots in Fig. 7(b)).

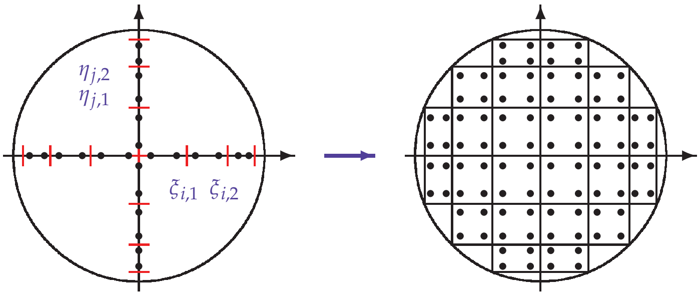

(a) (b)

Figure 7: Collocation points.

For a natural number M and $\tau=T/M$, let $\{t_n\}_{n=0}^M$ be a partition of $[0,T]$ such that $t_n=n\tau$, $n=0,\cdots,M$, and let $t_{n+1/2}=(t_n+t_{n+1})/2$, $n=0,\cdots,M-1$.

3.2 The approximate solution

For each t_n, $n=0,\cdots,M$, and each $\xi_{i,k}$, $i=1,\cdots,N-2$, $k=1,2$, the ADI OSC scheme involves finding the approximate solution $U^n_{i,k}$ which is a piecewise Hermite cubic (in the y variable) on $[y_{\gamma(i)},y_{N-\gamma(i)}]$ (see Fig. 8), where the function γ is defined by

$$\gamma(i)=\begin{cases} N/2-i, & \text{if } i=1,\cdots,N/2-1,\\ i-N/2+1, & \text{if } i=N/2\cdots,N-2.\end{cases} \tag{3.6}$$

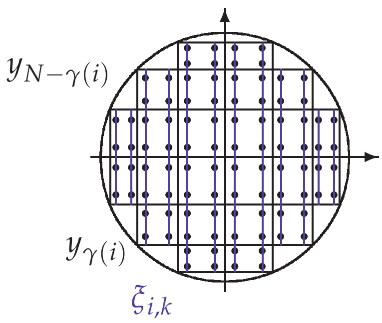

Figure 8: $U^n_{i,k}(y)\approx u(\xi_{i,k},y,t_n)$, $y\in[y_{\gamma(i)},y_{N-\gamma(i)}]$.

Also, for each $t_{n+1/2}$, $n=0,\cdots,M-1$, and each $\eta_{j,l}$, $j=1,\cdots,N-2$, $l=1,2$, the ADI OSC scheme involves finding the approximate solution $U^{n+1/2}_{j,l}$ which is a piecewise Hermite cubic (in the x variable) on $[x_{\gamma(j)},x_{N-\gamma(j)}]$ (see Fig. 9), where the function γ is defined in (3.6).

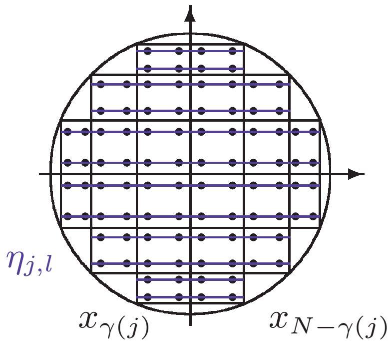

Figure 9: $U^{n+1/2}_{j,l}(x)\approx u(x,\eta_{j,l},t_{n+1/2})$, $x\in[x_{\gamma(j)},x_{N-\gamma(j)}]$.

3.3 The ADI OSC scheme

The ADI OSC scheme consists of the following three main steps (computations).

Step 1 Initial approximation.

At t_0, for each $\xi_{i,k}$, $i=1,\cdots,N-2$, $k=1,2$, the piecewise Hermite cubic $U^0_{i,k}$ on $[y_{\gamma(i)},y_{N-\gamma(i)}]$, with γ of (3.6), is determined by interpolating the values of $g_1(\xi_{i,k},\cdot)$ (cf. (3.2)) at the collocation points on the vertical line segment $\{\xi_{i,k}\}\times[y_{\gamma(i)},y_{N-\gamma(i)}]$ (see black dots in Fig. 10) and at the end points of the same vertical line segment (see green dots in Fig. 10).

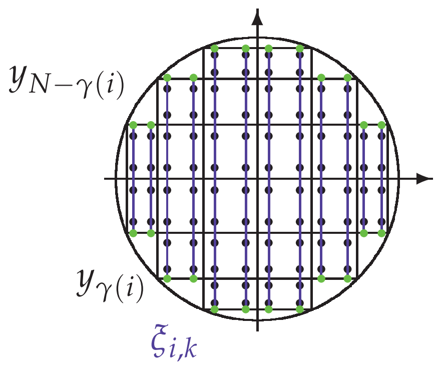

Figure 10: Initial approximation.

Step 2 Advancing from level t_n to level t_{n+1}.

To advance the approximate solution from time level t_n to t_{n+1}, $n=0,\cdots,M-1$, first, for each $\eta_{j,l}$, $j=1,\cdots,N-2$, $l=1,2$, we compute the piecewise Hermite cubic $U_{j,l}^{n+1/2}$ on $[x_{\gamma(j)},x_{N-\gamma(j)}]$, with γ of (3.6). $U_{j,l}^{n+1/2}$ satisfies the collocation equations

$$\begin{aligned}(2/\tau)\Big[U_{j,l}^{n+1/2}(\xi_{i,k})-U_{i,k}^{n}(\eta_{j,l})\Big]-(U_{j,l}^{n+1/2})_{xx}(\xi_{i,k})-(U_{i,k}^{n})_{yy}(\eta_{j,l})&\\ =f(\xi_{i,k},\eta_{j,l},t_{n+1/2}),\quad i=\gamma(j),\cdots,N-\gamma(j)-1,\quad k=1,2,&\end{aligned}$$

(cf. the first equation of (3.1) in [2]) and the two additional equations obtained by transferring the Dirichlet boundary condition (3.3) at the two boundary points $(x,y,t)=(\mp\sqrt{1-\eta_{j,l}^2},\eta_{j,l},t_{n+1/2})$ (see green dots in Fig. 11) to the left and right end points (see red dots in Fig. 11) of the horizontal line segment $[x_{\gamma(j)},x_{N-\gamma(j)}]\times\{\eta_{j,l}\}$. Each $U_{j,l}^{n+1/2}$ can be computed by solving the OSC TPBVP along the horizontal line segment at cost $\mathcal{O}(N-2\gamma(j))$.

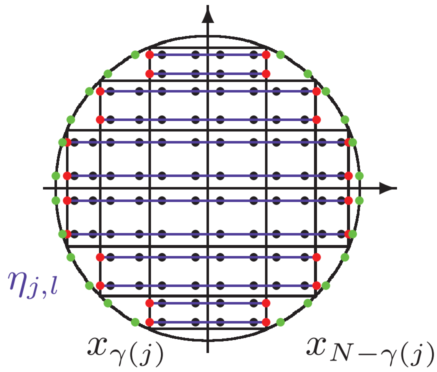

Figure 11: Advancing.

Next, for each $\xi_{i,k}$, $i=1,\cdots,N-2$, $k=1,2$, we compute the piecewise Hermite cubic $U_{i,k}^{n+1}$ on $[y_{\gamma(i)},y_{N-\gamma(i)}]$, with γ of (3.6). $U_{i,k}^{n+1}$ satisfies the collocation equations

$$\begin{aligned}(2/\tau)\Big[U_{i,k}^{n+1}(\eta_{j,l})-U_{j,l}^{n+1/2}(\xi_{i,k})\Big]-(U_{j,l}^{n+1/2})_{xx}(\xi_{i,k})-(U_{i,k}^{n+1})_{yy}(\eta_{j,l})&\\ =f(\xi_{i,k},\eta_{j,l},t_{n+1/2}),\quad j=\gamma(i),\cdots,N-\gamma(i)-1,\quad l=1,2,&\end{aligned}$$

(cf. the second equation of (3.1) in [2]) and the two additional equations obtained by transferring the Dirichlet boundary condition (3.3) at the two boundary points $(x,y,t)=(\xi_{i,k},\mp\sqrt{1-\xi_{i,k}^2},t_{n+1})$ (see green dots in Fig. 12) to the lower and upper end points (see red dots in Fig. 12) of the vertical line segment $\{\xi_{i,k}\}\times[y_{\gamma(i)},y_{N-\gamma(i)}]$. Each $U_{i,k}^{n+1}$ can be computed by solving the OSC TPBVP along the vertical line segment at cost $\mathcal{O}(N-2\gamma(i))$.

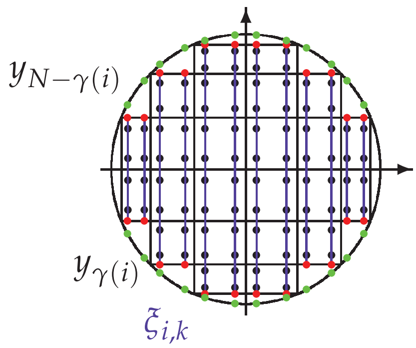

Figure 12: Advancing.

Step 3 The approximate solution U^M for $t=t_M=T$ on P_Ω.

From Step 2, for each $\xi_{i,k}$, $i=1,\cdots,N-2$, $k=1,2$, we know the piecewise Hermite cubic $U^M_{i,k}$ on $[y_{\gamma(i)},y_{N-\gamma(i)}]$, with γ of (3.6); (see Fig. 8). To determine the approximate solution U^M corresponding to $t=t_M=T$ and defined on the rectangular polygon P_Ω of (3.5), first, for each y_j, $j=1,\cdots,N/2-1$, we compute the piecewise Hermite cubic $U^M(\cdot,y_j)$ on $[x_{\gamma(j)},x_{N-\gamma(j)}]$ by interpolating the values $U^M_{i,k}(y_j)$, $i=\gamma(j),\cdots,N-\gamma(j)-1$, $k=1,2$, (see the corresponding blue dots in Fig. 13(a)) and by interpolating the values $g_2(\mp\sqrt{1-y_j^2},y_j,T)$ (see the corresponding green dots in Fig. 13(a)). In a similar way, for each y_j, $j=N/2+1,\cdots,N-1$, we compute the piecewise Hermite cubic $U^M(\cdot,y_j)$ on $[x_{\gamma(j-1)},x_{N-\gamma(j-1)}]$. For $j=N/2$, and hence $y_j=y_{N/2}=0$, we compute the piecewise Hermite cubic $U^M(\cdot,0)$ on $[x_1,x_{N-1}]$ by interpolating the values $U^M_{i,k}(0)$, $i=1,\cdots,N-2$, $k=1,2$, (see the corresponding blue dots in Fig. 13(a)) and by transferring the Dirichlet boundary condition (3.3) at the two boundary points $(x,y,t)=(\mp 1,0,T)$ (see green dots in Fig. 13(a)) to the left and right endpoints (see red dots in Fig. 13(a)) of

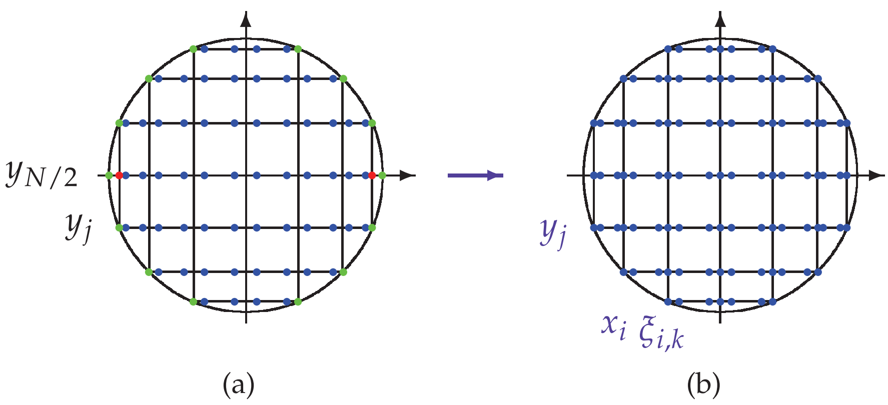

Figure 13: Approximate solution at $t=T$.

the horizontal line segment $[x_1,x_{N-1}]\times\{0\}$. Values of U^M at all points (x_i,y_j) and $(\xi_{i,k},y_j)$ in P_Ω (see blue dots in Fig. 13(b)) are stored.

Next, for each $\eta_{j,l}$, $j=1,\cdots,N-2$, $l=1,2$, we compute the piecewise Hermite cubic $U^M(\cdot,\eta_{j,l})$ on $[x_{\gamma(j)},x_{N-\gamma(j)}]$, with γ of (3.6), by interpolating the values $U^M_{i,k}(\eta_{j,l})$, $i=\gamma(j),\cdots,N-\gamma(j)-1$, $k=1,2$, (see the corresponding blue dots in Fig. 14(a)) and by transferring the Dirichlet boundary condition (3.3) at the two boundary points $(x,y,t)=(\mp\sqrt{1-\eta_{j,l}^2},\eta_{j,l},T)$ (see green dots in Fig. 14(a)) to the left and right end points (see red dots in Fig. 14(a)) of the horizontal line segment $[x_{\gamma(j)},x_{N-\gamma(j)}]\times\{\eta_{j,l}\}$. Values of U^M at all points $(x_i,\eta_{j,l})$ and $(\xi_{i,k},\eta_{j,l})$ in P_Ω (see blue dots in Fig. 14(b)) are stored.

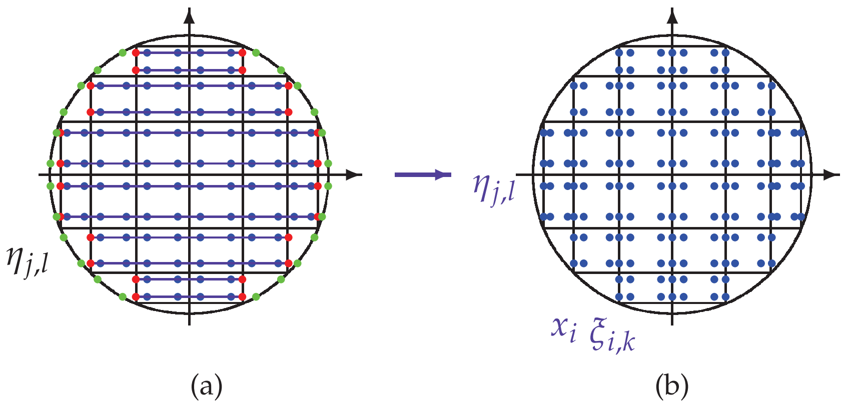

Figure 14: Approximate solution at $t=T$.

Thus, for any (x^*,y^*) in the rectangular polygon P_Ω, $U^M(x^*,y^*)$ is obtained by locating a cell of P_Ω containing (x^*,y^*) and calculating the 2d Lagrange interpolant [8, pp. 385] using the values of U^M at the 16 points in the cell (see 16 blue dots in Fig. 15).

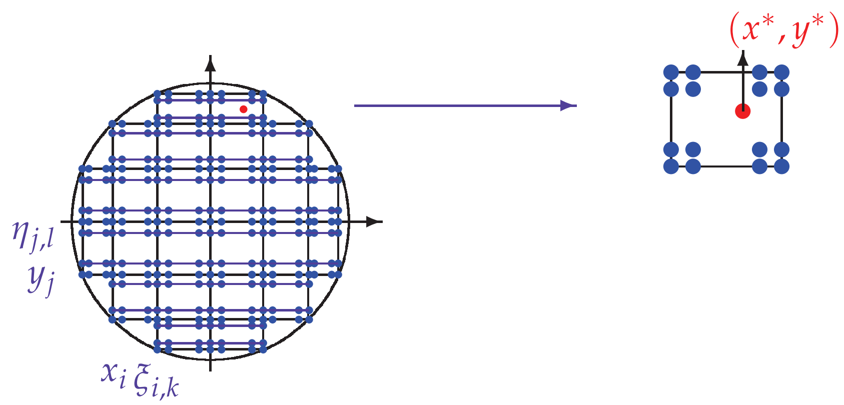

Figure 15: Approximate solution at $t=T$.

3.4 Numerical results

We solved the parabolic problem (3.1)-(3.3) with $u=e^{t+x+y}$ and $T=1$. For an even natural number N, we used partitions I and II corresponding to Figs. 5(a), (b) and Fig. 6, respectively. We computed the maximum norm error in U^M over the rectangular polygon P_Ω of (3.5) using 100 uniform points in each cell of P_Ω. We expected $\mathcal{O}(\tau^2)$ accuracy in t and $\mathcal{O}(h^4)$ accuracy in x,y, where

$$h=\max\Big\{\max_{i=1,\cdots,N-2}(x_{i+1}-x_i),\max_{j=1,\cdots,N-2}(y_{j+1}-y_j)\Big\}.$$

For partition I, h is given by (2.17). We set $\tau=1/N^2$ so that for large N, by (2.17), $\tau^2=1/N^4\approx h^4/\pi^4$, that is, τ^2 is approximately proportional to h^4 with the proportionality constant π^{-4}. For several values of N, denoted by N_i, and the corresponding values of h, denoted by h_i, we computed the convergence rate using the formula in (2.18), where ϵ_i was the error corresponding to N_i. The obtained results, presented in Table 2, indicate the expected convergence rate of 4 in the approximation U^M with respect to x and y.

Table 2: Errors and rates.

	$\lvert u(\cdot,T)-U^M\rvert$	
N_i	Error	Rate
10	9.80–04	
20	1.10–04	3.215
30	2.34–05	3.836
40	7.45–06	3.989
50	3.04–06	4.028

For partition II, it is clear from Fig. 6 that $h=y_{N/2+1}-y_{N/2}=y_{N/2+1}$, since $y_{N/2}=0$. Using the second equation in (3.4) with $j=N/2-1$, we obtain

$$h=y_{N/2+1}=\sqrt{1-(N-2)^2/N^2}\approx 2/\sqrt{N}\ \text{for}\ N\ \text{large}.$$

We therefore set $\tau=1/N$ so that $\tau^2=1/N^2\approx h^4/16$, that is, τ^2 is again approximately proportional to h^4 but with the proportionality constant $1/16$. The convergence rates in Table 3 were calculated in the same way as for Table 2. Once again the expected convergence rate of 4 is seen approximately. Since τ^2 and h^4 are proportional to one another,

Table 3: Errors and rates.

	$\lvert u(\cdot,T)-U^M\rvert$	
N_i	Error	Rate
10	2.24–01	
20	7.26–02	3.527
30	3.47–02	3.809
40	2.02–02	3.875
50	1.32–02	3.909

the error goes to 0 like $\mathcal{O}(\tau^2)=\mathcal{O}(1/N^2)$, that is, convergence is quadratic with respect to $1/N$. This explains why the errors in Table 3 are larger than the corresponding errors in Table 2.

4 Concluding remarks

We developed a simple approach to formulate an ADI OSC scheme for parabolic problems on some non-rectangular regions. The approach avoids using a conformal mapping of a region onto a rectangle.

Several extensions are yet to be considered such as extension to more general regions, variable coefficient and nonlinear parabolic problems, higher degree piecewise polynomials, other types of problems, such as second order hyperbolic problems, systems of parabolic equations, and three dimensional parabolic problems.

For an arbitrary region, it may not always be possible to construct a consistent nonuniform partition as shown for the unit disc in Section 3.1. Hence a generalization of our ADI OSC scheme for arbitrary domains will be considered using inconsistent partitions which are uniform in both coordinate directions.

Acknowledgments

This work was supported by grant no. 13328 from the Petroleum Institute, Abu Dhabi, UAE.

References

[1] B. Bialecki and R. I. Fernandes, *An orthogonal spline collocation alternating direction implicit Crank-Nicolson method for linear parabolic problems on rectangles*, SIAM J. Numer. Anal., 36 (1999), pp. 1414–1434.

[2] B. Bialecki and R. I. Fernandes, *An alternating-direction implicit orthogonal spline collocation scheme for nonlinear parabolic problems on rectangular polygons*, SIAM J. Sci. Comput., 28 (2006), pp. 1054–1077.

[3] B. L. Buzbee, F. W. Dorr, J. A. George and G. H. Golub, *The direct solution of the discrete Poisson equation on irregular regions*, SIAM J. Numer. Anal., 8 (1971), pp. 722–736.

[4] J. C. Diaz, G. Fairweather and P. Keast, FORTRAN *packages for solving certain almost block diagonal linear systems by modified alternate row and column elimination*, ACM Trans. Math. Software, 9 (1983), pp. 358–375.

[5] J. C. Diaz, G. Fairweather and P. Keast, *Algorithm 603 COLROW and ARCECO: FORTRAN packages for solving certain almost block diagonal linear systems by modified alternate row and column elimination*, ACM Trans. Math. Software, 9 (1983), pp. 376–380.

[6] J. Douglas, Jr. and T. Dupont, *Collocation methods for parabolic equations in a single space variable*, Lecture Notes in Mathematics, 385 (1974), Springer-Verlag, New York.

[7] R. I. FERNANDES, B. BIALECKI AND G. FAIRWEATHER, *Alternating direction implicit orthogonal spline collocation methods for evolution equations*, Mathematical Modelling and Applications to Industrial Problems (MMIP-2011), M. J. Jacob and S. Panda, eds., Macmillan Publishers India Ltd., 2012, pp. 3–11.
[8] D. KINCAID AND W. CHENEY, Numerical Analysis, Brooks/Cole Publishing Company, California, 1991.
[9] D. W. PEACEMAN AND H. H. RACHFORD, JR., *The numerical solution of elliptic and parabolic differential equations*, J. Soc. Indust. Appl. Math., 3 (1955), pp. 28–41.